oligosaccharide portions of these molecules in Me_2SO and Me_2NCHO. In these studies, the amide side chain (in GalNAcβ(1→3)Gal) was found to exist in two conformations basically involving torsions about the trans arrangement (τ = 160° and 60°). In this report we have shown by comparing experimental and simulated NOEs from the NH proton that for the oligosaccharides LND-1 and LNF-1 only one of these two conformations agrees with experiment.

Low-Temperature, Cooperative Conformational Transition within [Zn-Cytochrome *c* Peroxidase, Cytochrome *c*] Complexes: Variation with Cytochrome

Judith M. Nocek,[†] Eric D. A. Stemp,[†] Michael G. Finnegan,[‡] Thomas I. Koshy,[§] Michael K. Johnson,[‡] E. Margoliash,[§] A. Grant Mauk,[⊥] Michael Smith,[⊥] and Brian M. Hoffman*,[†]

Contribution from the Departments of Chemistry and Biochemistry, Molecular Biology, and Cell Biology, Northwestern University, Evanston, Illinois 60208, Department of Chemistry, University of Georgia, Athens, Georgia 30602, and Department of Biochemistry, University of British Columbia, Vancouver, British Columbia, Canada V6T 1Z3. *Received January 7, 1991*

Abstract: Conformational dynamics within the complex between Zn-substituted cytochrome *c* peroxidase (ZnCcP) and cytochrome *c* (Cc) has been studied by examining the quenching of the ^{3}ZnP excited state by the ferriheme of Cc. The temperature and solvent dependence of the triplet-state quenching rate constants (k_q) show that complexes of ZnCcP with a large set of Fe^{3+} cytochromes *c* undergo a transition between a low-temperature state that does not exhibit triplet quenching and a high-temperature state that does. Within the narrow transition range (220 K < *T* < 250 K), the decay traces for the [ZnCcP, Fe^{3+}Cc] complexes are nonexponential, and outside of this range they are exponential. This behavior is displayed by complexes with Cc(*Drosophila melanogaster*), Cc(*Candida krusei*) and a suite of site-directed mutants of Cc(yeast iso-1) where position 82 contains either an aliphatic (Met, Ser, Leu, or Ile) or an aromatic (Phe) residue. Above 250 K, k_q varies strongly among these complexes and decreases sharply with the concentration of cosolvent (EG = ethylene glycol), apparently because of increasing viscosity, while both the breadth of the transition range and its midpoint vary little within this class. MCD and optical spectra between ambient and 4 K rule out the trivial explanation that the transition might reflect changes in the coordination state, and the invariance of k_q with a 10-fold increase in [Cc] shows that the proteins remain bound as a complex upon cooling. As the midpoint and breadth of the transition are unaffected by changes in percent EG, the transition does not appear to arise from a solvent-driven process. Instead, we propose that, at ambient temperatures, the binding interface of the [CcP, Cc] complex undergoes rapid dynamic rearrangements between the subset of conformers that exhibit ^{3}ZnP quenching and the subset that does not. Below the transition range, the complex exists in the latter form, and it is suggested that, upon heating, there is a cooperative loosening of the binding interactions within the interface. We present an heuristic description of the complex based on the statistical mechanical description of the cooperative helix-coil transition in poly(amino acids). In contrast, members of a second class of complexes, those with Cc(horse), Cc(tuna), and Cc(rat), have low quenching rate constants ($k_q \approx 40$ s^{-1} at ambient) that decrease smoothly to $k_q \approx 0$ s^{-1} by 250 K. Furthermore, k_q for these complexes shows little dependence upon either solvent or cytochrome, and the triplet decay traces remain exponential at all temperatures.

Introduction

In this paper, conformational dynamics within the complex between Zn-substituted cytochrome *c* peroxidase (ZnCcP) and cytochrome *c* (Cc) has been studied by examining the quenching of the ^{3}ZnP excited state by the ferriheme of Cc.[1-3] This complex is particularly well suited for such studies for several reasons. At low ionic strengths, the complex forms with a large protein association constant ($K_a = 10^7$ M^{-1})[4] and a model for the physiological complex has been generated[5] from the crystal structures of Fe^{3+}Cc(tuna) and Fe^{3+}CcP from *Saccharomyces cerevisiae*. In addition, cytochromes *c* from numerous species, as well as site-directed mutants of both Cc and CcP provide a wealth of complexes with which to probe the effects of structure on protein dynamics.[6,7]

In the proposed model for the [Fe^{3+}CcP, Fe^{3+}Cc(tuna)] complex, generated by optimizing the electrostatic interactions between complementary surface charges on the two proteins, the complex is held together by electrostatic interactions between positively charged residues near the exposed heme crevice of Cc (Lys 13, 27, 72, 86, and 87) and negatively charged residues on the surface

[†] Department of Chemistry, Northwestern University.
[‡] Department of Chemistry, University of Georgia.
[§] Department of Biochemistry, Molecular Biology, and Cell Biology, Northwestern University.
[⊥] Department of Biochemistry, University of British Columbia.

(1) Examples of conformational gating within hemoproteins include (a) Yuan, X.; Songcheng, S.; Hawkridge, F. M. *J. Am. Chem. Soc.* **1990**, *112*, 5380-5381. (b) Isied, S. S. In *Electron Transfer in Biology and the Solid State*; Johnson, M. K., et al., Eds.; American Chemical Society: Washington, DC, 1990; pp 91-100.
(2) Examples of conformational gating within electrostatic complexes include (a) Peerey, L. M.; Kostic, N. *Biochemistry* **1989**, *28*, 1861-1868. (b) Morand, L. Z.; Frame, M. K.; Colvert, K. K.; Johnson, D. A.; Krogmann, D. W.; Davis, D. J. *Biochemistry* **1989**, *28*, 8039-8047. (c) Pan, L. P.; Frame, M.; Durham, B.; Davis, D.; Millet, F. *Biochemistry* **1990**, *29*, 3231-3236.
(3) Examples of conformational gating within [CcP, Cc] complexes include (a) Hazzard, J. T.; Poulos, T. L.; Tollin, G. *Biochemistry* **1987**, *26*, 2836-2848. (b) Cheung, E.; English, A. M. *Inorg. Chem.* **1988**, *27*, 1078-1081.
(4) (a) Erman, J. E.; Vitello, L. B. *J. Biol. Chem.* **1980**, *255*, 6224-6227. (b) Nicholls, P.; Mochan, E. *Biochem. J.* **1971**, *121*, 66-67. (c) Mochan, E.; Nicholls, P. *Biochim. Biophys. Acta* **1972**, *267*, 309-319. (d) Vitello, L. B.; Erman, J. E. *Arch. Biochem. Biophys.* **1987**, *258*, 621-629.
(5) Poulos, T. L.; Kraut, J. *J. Biol. Chem.* **1980**, *255*, 10322-10330.
(6) Liang, N.; Mauk, A. G.; Pielak, G. J.; Johnson, J. A.; Smith, M.; Hoffman, B. M. *Science* **1988**, *240*, 311-313.
(7) Ho, P. S.; Sutoris, C.; Liang, N.; Margoliash, E.; Hoffman, B. M. *J. Am. Chem. Soc.* **1985**, *107*, 1070-1071.

0002-7863/91/1513-6822$02.50/0

of CcP (Asp 37, 79, and 216). In this structure, the hemes are nearly parallel with an edge separation of ~16.5 Å. Although a similar binding geometry has been inferred from the results of chemical modification studies, electrostatic calculations suggest that at least two other nearby sites are available.[8] Fluorescence quenching measurements,[9] gel filtration studies,[10,11] and CO recombination experiments[12] all suggest the existence of multiple binding sites.

Examination of triplet-state quenching within the complex of ZnCcP with yeast iso-1 Cc disclosed that the complex undergoes a remarkable transition having a midpoint near 235 K and a breadth of only ~30 K.[13] Triplet decay curves within this range show nonexponential kinetics, which indicates that the complex exhibits multiple conformational forms with different decay constants and that the rate of interconversion among conformers is competitive with or slower than the rate of triplet decay. To elucidate the structural basis for this transition, we now report full characterization of the kinetics for triplet-state quenching as a function of temperature and solvent using complexes with Cc isolated from a variety of organisms, as well as variants of Cc(yeast iso-1) that have been mutated at the evolutionarily conserved, interfacial residue 82.

Materials and Methods

Protein Isolation. Native Fe^{3+}CcP, isolated from Baker's yeast (Red Star) according to the procedure of Nelson et al.[14] with the modifications suggested by English et al.[15] gave a purity index (A_{408}/A_{280}) of 1.25–1.30 in 0.1 M KPi at pH 7, and heme was extracted from the acidified protein into 2-butanone (spectrophotometric-grade, Aldrich) according to the protocol of Yonetani.[16] The apoprotein was then reconstituted with ZnP (Porphyrin Products, Logan, UT) and purified chromatographically on DEAE Sepharose CL-6B. Purity of the Zn-substituted peroxidase was assayed by isoelectric focusing (Pharmacia Phast System with polyacrylamide gels) and spectrally ($A_{432}/A_{280} \geq 3.0$ in 10 mM potassium phosphate buffered at pH 7), and concentrations were determined by using ϵ_{432}(ZnCcP) = 180 mM^{-1} cm^{-1}.

Cytochromes *c* from horse,[17] tuna,[17] and rat[18] were prepared as described previously. Cc(*Candida krusei*) was purchased from Sigma (type VII) and used without further purification. The recombinant Cc(*Drosophila melanogaster*) was expressed in yeast and is a mixture comprising proteins that are un-, mono-, di-, and trimethylated at Lys 72.[19] Position 82 [based on the sequence numbering for Cc(tuna)] mutants of Cc(yeast iso-1) from *S. cerevisiae* were prepared as described previously.[20,21] These included proteins where Phe 82 has been replaced with Ser, Met, Leu, or Ile. To prevent dimerization and autoreduction, Cys 102 in each of these mutants was mutated to Thr. The Cc(C102T) mutant, which retains Phe at position 82, is taken as representative of the wild type (WT) Cc(yeast iso-1) protein, and the background C102T mutation is not explicitly noted below when mutations at position 82 are indicated. Cc was assayed in aqueous buffer by using $\epsilon_{410}(Fe^{3+}Cc)$ = 106.1 mM^{-1} cm^{-1}.[22]

Position 82 mutants of Cc(yeast iso-1) were oxidized with $(NH_4)[Co(dipic)_2]$ and then purified by FPLC using a Mono-S anion exchange column; excess oxidant was removed by extensive washing with low-salt buffer prior to elution off the FPLC column. These mutant cytochromes were exchanged into 10 mM, pH 7 potassium phosphate buffer (KPi) by using Centricon 10 microconcentrators. Cytochromes *c* from other species also were oxidized to the Fe^{3+} form with a large excess of $(NH_4)[Co(dipic)_2]$. All cytochromes *c* were concentrated to ~0.3 mM and stored in liquid nitrogen as frozen pellets.

Cryosolvent Preparation. Cryosolvents were made to the desired composition by first mixing appropriate volumes of ethylene glycol (EG) and deionized water. Then, stock solutions of Pi (KH_2PO_4 and K_2HPO_4) were prepared by dissolving the salts in the desired cryosolvent; potassium salts were used because pH changes during cooling are less for KPi buffer than for NaPi buffer.[23] The cryobuffer was adjusted to pH 6 (4 °C) by titrating the stock monobasic KPi with stock dibasic KPi. Low concentrations of buffers (10 mM KPi at pH 6, unless stated otherwise) were used to optimize the electrostatic binding between the two proteins. Similar procedures were followed with glycerol (GlOH). Unless otherwise stated, kinetic measurements were made with 30% EG; variable-temperature optical measurements and MCD measurements were made with 60% EG cryobuffer because this solvent remains optically clear down to low temperatures. Addition of buffer and protein to these solvents lowers the freezing transition by 5–10 K from their published glassing points, which for EG cryosolvents are 15%, ~266 K; 30%, ~256 K; 45%, ~238 K; 60% ~204 K.[24]

Preparation of [ZnCcP, Cc] Complexes. For low-temperature measurements, aqueous stock solutions of preformed [ZnCcP, Fe^{3+}Cc] complexes were diluted into cryobuffers. This procedure is necessary because ZnCcP, when uncomplexed, is unstable in cryobuffer, even with low concentrations of cosolvent. The stock solutions were formed by mixing solutions of ZnCcP and Fe^{3+}Cc to give A_{408}/A_{432} = 1.4 (0.3), which corresponds to a molar ratio of Cc/CcP = 2.5 (0.3). Because dioxygen is an efficient quencher of ^{3}ZnP, all samples were prepared in Schlenck-type optical cells with two stopcocks. Quartz rather than Pyrex cuvettes were used because the latter gave long-lived luminescent signals. To minimize breakage during the cooling experiments, cells with 0.4-cm path length were used. The cryobuffer was flushed with nitrogen for at least 20 min and then added to the cell under positive nitrogen pressure by using gastight syringes (Hamilton). Full anaerobicity was achieved by adding an enzymatic oxygen scavenging system[25] (final concentrations: 100 μg/mL glucose oxidase; 25 μg/mL catalase; and 10 mM glucose). Lastly, an aliquot of the preformed complex was added to yield a final concentration of 2–10 μM.

To prepare the [ZnCcP, Fe^{2+}Cc] complex, a sample of a [ZnCcP, Fe^{3+}Cc] complex in cryobuffer was reduced by the addition of a 100-fold excess of 2-mercaptoethanol under nitrogen. Reduction to the [ZnCcP, Fe^{2+}Cc] state was complete within 1 h, as ascertained by monitoring the growth of the α-band at 550 nm (ϵ_{550} = 29 mM^{-1} cm^{-1} [26]) and the red shift of the Soret peak for Cc to 416 nm.

Instrumentation. Optical spectra were obtained with a single-beam, diode-array spectrophotometer (Hewlett-Packard 8451) having 2-nm resolution. Luminescence spectra at ambient were obtained in the laboratory of Prof. Laszlo Lorand by using an Aminco SLM 8000C photon-counting spectrofluorometer. Samples were irradiated at 432 nm and collected over a 0.1-s integration time.

Triplet states of the [ZnCcP, Cc] complexes were produced by irradiating the samples with either a Xenon Corp. micropulser assembly (Model 457 with an N-722D flashtube; 5 J/pulse) or a photoflash (Sunpak, Model 611), which was filtered through narrow band interference filters to give excitation at 430 ± 10 nm (Oriel Corp., 53815). Emission at λ ≥ 700 nm was collected after passage through a broad-band, long-pass filter (Oriel Corp., 57893). When the xenon flash was used, the signal-to-noise ratio was improved by averaging 50–100 signals. Data acquisition was controlled by a PC-clone interfaced to a 10-MHz transient digitizer (Wavesaver 10v3, Epic Instruments); 500 pretrigger and 2048 data points were collected. Typically the 2048 data points were averaged and binned into 250 points prior to curve fitting. The algorithm of Marquardt was applied for nonlinear least-squares analysis.[27]

(8) (a) Northrup, S. H.; Boles, J. O.; Reynolds, J. C. L. *Science* **1988**, *241*, 67–70. (b) Northrup, S. H.; Boles, J. O.; Reynolds, J. C. L. *J. Phys. Chem.* **1987**, *91*, 5991–5998.
(9) Kornblatt, J. A.; English, A. M. *Eur. J. Biochem.* **1986**, *155*, 505–511.
(10) Margoliash, E.; Ferguson-Miller, S.; Kang, C. H.; Brautigan, D. L. *Fed. Proc.* **1976**, *35*, 2124–2130.
(11) Kang, C. H.; Ferguson-Miller, S.; Margoliash, E. *J. Biol. Chem.* **1977**, *252*, 919–926.
(12) Ho, P. S. Ph.D. Thesis, Northwestern University, 1984.
(13) Nocek, J. M.; Liang, N.; Wallin, S. A.; Mauk, A. G.; Hoffman, B. M. *J. Am. Chem. Soc.* **1990**, *112*, 1623–1625.
(14) Nelson, C. E.; Sitzman, E. V.; Kang, C. H.; Margoliash, E. *Anal. Biochem.* **1977**, *83*, 622–631.
(15) English, A. M.; Laberge, M.; Walsh, M. *Inorg. Chim. Acta* **1986**, *123*, 113–116.
(16) Yonetani, T. *J. Biol. Chem.* **1967**, *242*, 5008–5013.
(17) Brautigan, D. L.; Ferguson-Miller, S.; Margoliash, E. *Methods Enzymol.* **1978**, *53*, 128–164.
(18) Luntz, T. R.; Schejter, A.; Garber, E. A. E.; Margoliash, E. *Proc. Natl. Acad. Sci. U.S.A.* **1989**, *86*, 3524–3528.
(19) Koshy, T. I.; Luntz, T. L.; Schejter, A.; Margoliash, E. *Proc. Natl. Acad. Sci. U.S.A.* **1990**, *87*, 8697–8701.
(20) Cutler, R. L.; Pielak, G. J.; Mauk, A. G.; Smith, M. *Protein Eng.* **1987**, *1*, 95–99.
(21) Pielak, G. J.; Mauk, A. G.; Smith, M. *Nature* **1985**, *313*, 152–154.
(22) Margoliash, E.; Frohwirt, N.; Wiener, E. *Biochem. J.* **1959**, *71*, 559–572.
(23) (a) Orii, Y.; Morita, M. *J. Biochem.* **1977**, *81*, 163–168. (b) Williams-Smith, D. L.; Bray, R. C.; Barber, M. J.; Tsopanakis, A. D.; Vincent, S. P. *Biochem. J.* **1977**, *167*, 593–600. (c) Van den Berg, L.; Rose, D. *Arch. Biochem. Biophys.* **1959**, *81*, 319–329.
(24) Douzou, P. *Cryobiochemistry: An Introduction*; Academic Press: New York, 1977.
(25) Stankovich, M. T.; Schopfer, L. M.; Massey, V. *J. Biol. Chem.* **1978**, *253*, 4971–4979.
(26) Yonetani, T.; Ray, G. S. *J. Biol. Chem.* **1965**, *240*, 4503–4508.
(27) Bevington, P. R. *Data Reduction and Error Analysis for the Physical Sciences*; McGraw-Hill: New York, 1969; pp 134–186.

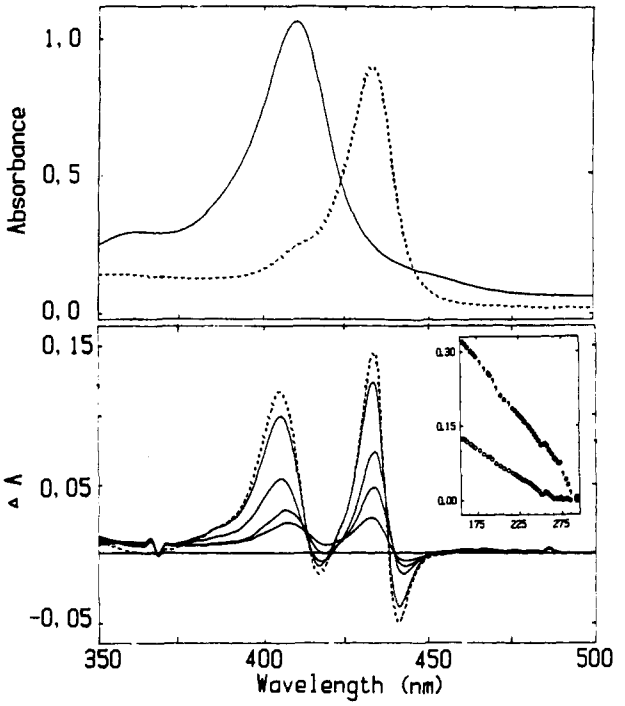

Figure 1. Optical spectra for the [ZnCcP, Fe^{3+}Cc(F82L)] complex in the Soret region. Upper: Ambient-temperature spectra of 10 μM Fe^{3+}Cc(F82L) (—) and 5.0 μM ZnCcP (---) in 10mM KPi (pH 6) buffer. Lower: Difference spectra for the [ZnCcP, Fe^{3+}Cc(F82L)] complex at reduced temperatures obtained by subtracting the 291 K spectrum. Traces are shown at 291, 273, 248, 223, 173, and 143 K (---). Inset: Relative absorbance differences $[(A_T - A_{291})/A_{291}]$ for the Soret peaks of ZnCcP [432 nm, (●)] and Fe^{3+}Cc(F82L) [406 nm (○)] within the [ZnCcP, Cc] complex. Conditions: 3.8 μM ZnCcP, 9.8 μM Cc; 60% EG/10 mM KPi, pH 6 at ambient.

MCD spectra were recorded with a Jasco J500C spectropolarimeter fitted with a Jasco MCD 1B electromagnet (0–1.5 T) for room temperature measurements or an Oxford Instruments SM3 superconducting magnet (0–5 T) for variable-temperature, high-field measurements. Details of the MCD instrumentation and the experimental protocols used for variable-temperature MCD measurements have been described elsewhere.[28]

Temperature Control. Low-temperature optical spectra and luminescence signals were collected by using a dewar having quartz windows (W. A. Sales, Ltd.). Temperature was regulated by adjusting the flow of cold nitrogen gas from boiling liquid nitrogen and read with a type K, Chromel-alumel thermocouple (Fluke, Model 51K thermometer) fastened to the sample cuvette. Measurements were obtained at 1–3 °C temperature intervals, and during a measurement, the temperature was maintained to within ±0.2 °C. The data reported here were collected as samples were cooled slowly (20 K/h) to 200 K, whereupon the cooling rate was increased to ~60 K/h. To check for hysteresis, measurements also were made while the sample was warmed from 77 K. Although the temperature could not be regulated as well when data were so obtained, the warming and cooling curves match rather well, with shifts of only ca. 5 K that are at least in part due to a lack of thermal equilibrium between sample and sensor.

Results

Spectral Properties. The Soret region of the optical spectra of [ZnCcP, Cc] complexes in aqueous solution is the sum of the spectra of the two individual proteins. The Soret peak of Fe^{3+}Cc falls at 408 nm, whereas that of ZnCcP falls at 432 nm (Figure 1, upper). Near pH 7, the Fe heme of Cc is ligated by Met 80 and His 18,[29] and the optical spectrum of ZnCcP at ambient indicates that the Zn is 5-coordinate, with the fifth ligand undoubtedly being His 175.[30,31]

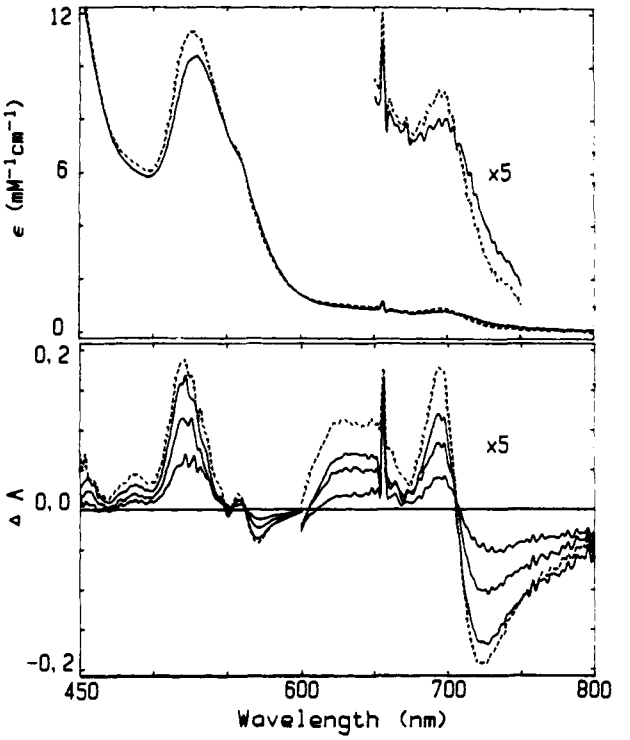

Figure 2. Variable-temperature optical spectra for Fe^{3+}Cc(*C. krusei*) in the visible region. Upper: Spectra at 297 K (—) and 200 K (---). Lower: Difference spectra obtained by subtracting the 297 K spectrum. Traces are shown at 297, 273, 248, 223, and 200 K (---). Conditions: 0.39 mM Cc; 60% EG/10 mM KPi, pH 6 at ambient.

When the complex is preformed in aqueous buffer and diluted into cryobuffer, the ratio of extinction coefficients, $\epsilon_{408}/\epsilon_{432}$, increases relative to aqueous buffer but the Soret bands of Fe^{3+}Cc and ZnCcP do not shift significantly and are invariant with time. The triplet decay rate constant is lower in cryobuffer than in aqueous buffer (vide infra), but is again time invariant. Thus, the [ZnCcP, Cc] complex is stable in the cryobuffer. However, when ZnCcP is added to EG in the absence of Cc, its Soret maximum broadens with time and the triplet decay rate increases to $\geq 400\ s^{-1}$. We attribute this to loss of ZnP from the uncomplexed ZnCcP in cryosolvent. The fact that complex formation protects the ZnCcP in cryobuffer provides strong evidence that the cryosolvent does not induce dissociation of the complex.

UV–vis and MCD spectroscopies have been used to check for any strong perturbation of the coordination geometry of either Cc or ZnCcP in cryosolvent at lower temperatures. Optical spectra of the [ZnCcP, Fe^{3+}Cc(F82L)] complex in 60% EG between room temperature and 155 K are shown in Figure 1 (lower) as difference spectra obtained by subtracting the 298 K spectrum. As the sample is cooled, the intensity of the Soret peak for Fe^{3+}Cc(F82L) (406 nm) sharpens slightly (by 150 K, its amplitude has increased by 14%) but, within the 2-nm resolution of the spectrometer, the peak does not shift. The peak for ZnCcP at 432 nm also sharpens smoothly without shifting upon cooling (32% increase in amplitude by 150 K).

The absence of a shift in the Soret peak of ZnCcP shows that the Zn^{2+} of ZnCcP remains 5-coordinate even at 77 K, consistent with the known coordination preference of ZnP.[30,31] However, in alkaline solution, the Met 80 ligand of Fe^{3+}Cc is replaced by a new strong-field ligand,[32] and this alkaline transition generally does not perturb the Soret spectrum of Cc. The pK_a for the alkaline transition is reported to be species-dependent: For Cc(horse), the transition has a pK_a of 9.1, whereas for Cc(yeast iso-1)

(28) Johnson, M. K. In *Metal Clusters in Proteins*; Que, L., Jr., Ed.; American Chemical Society: Washington, DC, 1988; pp 326–342.
(29) Swanson, R.; Trus, B. L.; Mandel, N.; Mandel, G.; Kallai, O. B.; Dickerson, R. E. *J. Biol. Chem.* **1977**, *252*, 759–775.
(30) Wang, M. R.; Hoffman, B. M. *J. Am. Chem. Soc.* **1984**, *106*, 4235–4240.
(31) Gouterman, M. In *The Porphyrins*; Dolphin, D., Ed.; Academic Press: New York, 1978; Vol. III, pp 1–165.
(32) (a) Brautigan, D. L.; Feinberg, B. A.; Hoffman, B. M.; Margoliash, E.; Peisach, J.; Blumberg, W. E. *J. Biol. Chem.* **1977**, *252*, 574–582. (b) Bosshard, H. R. *J. Mol. Biol.* **1981**, *153*, 1125–1149.

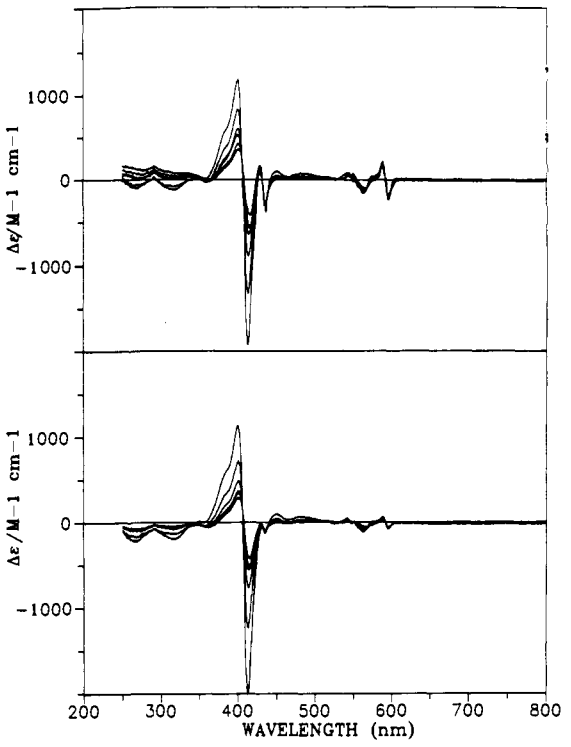

Figure 3. Variable-temperature MCD spectra for [ZnCcP, Fe^{3+}Cc-(WT)] and [ZnCcP, Fe^{3+}Cc(horse)] complexes. Upper: [ZnCcP, Fe^{3+}Cc(WT)]; 0.035 mM in ZnCcP and 0.086 mM in Fe^{3+}Cc. Temperatures, 65, 103, 168, 228, 256, and 300 K; magnetic field, 4.5 T. Lower: [ZnCcP, Fe^{3+}Cc(horse)]; 0.052 mM in ZnCcP and 0.205 mM in Fe^{3+}Cc. Temperatures, 50, 96, 170, 200, 257, and 298 K; magnetic field, 4.5 T. MCD intensity increases with decreasing temperature. Extinction coefficients were based on [Cc]. Samples were prepared in 60% EG/10 mM KPi, pH 6 cryobuffer.

it occurs at 8.5, and among the Phe 82 mutants the pK_a ranges from 8.5 for Cc(WT) to a low of 7.2 for Cc(F82L).[33] Given that the pH of 50% EG/10 mM KPi cryobuffer increases from pH 6 at ambient to pH 7.1 at 233 K,[24] the possibility of heme–ligand exchange is real, and thus the smooth change in the intensity of the Soret bands (Figure 1) is not conclusive. However, the 695-nm band of Cc is diagnostic of the Met–His coordination geometry; it disappears as the pH is raised through the alkaline transition region. To test specifically whether the alkaline transition is induced during cooling, we monitored the intensity of the 695-nm band of Fe^{3+}Cc(*C. krusei*) in 60% EG between 200 and 300 K. Figure 2 shows the optical spectra for Cc(*C. krusei*) at 200 and 297 K (upper), and the difference spectra obtained by subtracting the 297 K spectrum (lower). We find that the 695-nm band sharpens slightly (14% increase in amplitude) without a significant shift in position. Thus, we infer that the Met–His coordination geometry is maintained upon cooling to 200 K.

Variable-temperature MCD spectroscopy was also used to verify the axial ligation of the cytochromes (and of ZnCcP) at low temperatures. Gadsby et al.[34] have shown that low-temperature MCD spectroscopy can be used to monitor the alkaline transition in Fe^{3+}Cc(horse) via changes in the pattern of bands in the visible region and the loss of the feature at 695 nm that is indicative of Met–His axial ligation. Room temperature MCD spectra of the [ZnCcP, Fe^{3+}Cc(WT)] complex were identical in the aqueous and cryobuffer solutions (data now shown), confirming that 60% EG does not alter the ligation state of either protein. Figure 3 shows the MCD spectra for the [ZnCcP, Fe^{3+}Cc(horse)] and [ZnCcP, Fe^{3+}Cc(WT)] complexes in 60% EG at temperatures in the range 50–300 K. The dominant temperature-dependent band centered

(33) Pearce, L. L.; Gartner, A. L.; Smith, M.; Mauk, A. G. *Biochemistry* **1989**, *28*, 3152–3156.
(34) Gadsby, P. M. A.; Peterson, J.; Greenwood, C.; Thomson, A. J. *Biochem. J.* **1987**, *246*, 43–54.

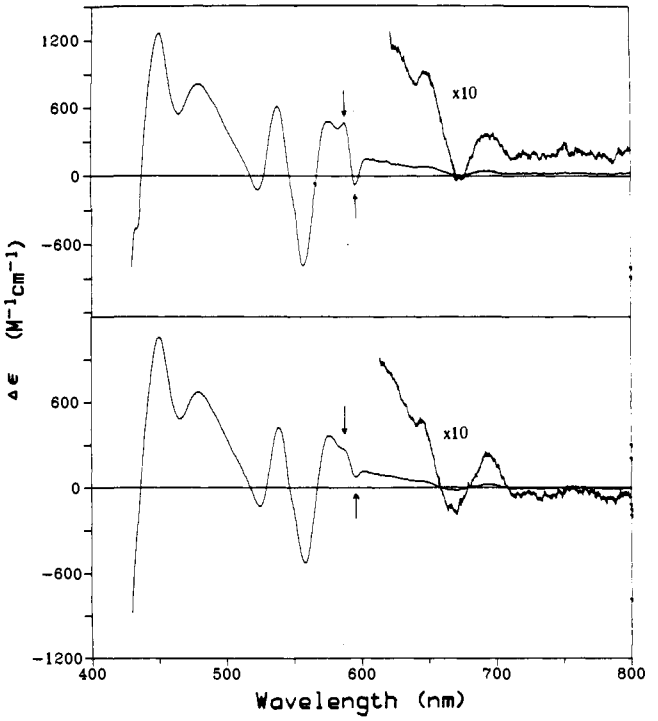

Figure 4. 4.2 K MCD spectra for the [ZnCcP, Cc(WT)] (upper) and [ZnCcP, Fe^{3+}Cc(horse)] (lower) complexes in 60% EG/10mM KPi, pH 6 cryobuffer. Samples and magnetic fields as described in Figure 3. Arrows indicate temperature-independent features arising from ZnCcP.

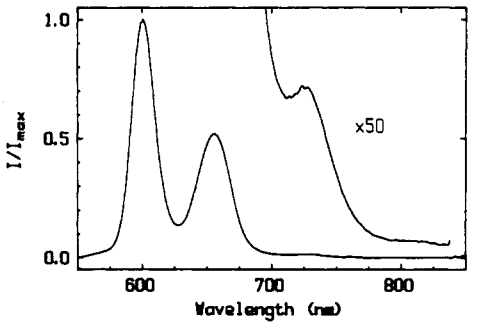

Figure 5. Luminescence spectrum for ZnCcP in aqueous buffer. Conditions: 3.3 μM ZnCcP; 10 mM KPi; pH 6; excitation wavelength, 432 nm; integration time 100 ms; T = 299 K.

at 406 nm arises from the paramagnetic ($S = {}^1/_2$) low-spin Fe^{3+}Cc, whereas the weak, temperature-independent, derivative-shaped bands centered at 432 and 590 nm originate from the diamagnetic ZnCcP. The absence of significant frequency shifts in these bands as a function of temperature confirms that the ligation states of both proteins remain unchanged as a function of temperature in the range of 50–300 K.

Figure 4 shows MCD spectra measured at 4.2 K and 4.5 T for both the [ZnCcP, Fe^{3+}Cc(horse)] and [ZnCcP, Fe^{3+}Cc(WT)] complexes. With the exception of the derivative-shaped feature centered at 590 nm (indicated by arrows in Figure 4) that arises from diamagnetic ZnCcP, the bands are temperature dependent and are attributed exclusively to Fe^{3+}Cc. In both complexes, the pattern of bands and the presence of the weak feature at 695 nm are indicative of Met–His axial ligation of Fe^{3+}Cc. The intensity of the 695-nm band relative to the other spectral features shows that, in both samples, this coordination arrangement prevails for all the Fe^{3+}Cc (complexed or uncomplexed). Hence, the low-temperature MCD data provide definitive evidence for preservation of Met–His axial ligation of the Fe^{3+}Cc in both complexes upon cooling to 4.2 K.

The steady-state luminescence spectrum for ZnCcP at ambient is shown in Figure 5. For ZnCcP, fluorescence peaks are seen at 600 and 656 nm; the peak at 729 nm is attributed to phos-

phorescence, consistent with results reported by Koloczek et al.[35] Taking the 729-nm phosphorescence peak as the origin gives a singlet–triplet energy gap of 2950 cm^{-1} (8.43 kcal/mol).

Triplet-State Decay Kinetics for ZnCcP and [ZnCcP, Fe^{2+}Cc] Complexes. Time-resolved triplet decay traces were obtained by monitoring the luminescence of ZnCcP and the [ZnCcP, Fe^{2+}Cc] complexes in aqueous buffer for 270 K ≤ T ≤ 300 K and for the [ZnCcP, Fe^{2+}Cc] complexes in cryobuffer for 77 K ≤ T ≤ 300 K.[36] In all cases, the progress curves are exponential for ≥5 half-lives. The triplet decay rate constant for ZnCcP in aqueous buffer [k_d = 124 (6) s^{-1} at 293 K] is not increased by complexation with Fe^{2+}Cc, indicating the absence of energy-transfer or electron-transfer quenching by Fe^{2+}Cc. It is the same in all cryobuffers, which further indicates that the cryosolvent does not strongly perturb the heme pocket of ZnCcP. Nor is the complex dissociated in cryobuffer because in this case ZnP would have been expelled from uncomplexed ZnCcP, thereby causing the apparent rate constant to drastically increase (see above). Finally, the intrinsic rate constants for a variety of Fe^{2+}Cc are experimentally indistinguishable: e.g., at 293 K, k_d(WT) = 126 (4) s^{-1}; k_d (rat) = 111 s^{-1}; k_d(F82M) = 120 (3) s^{-1}; and k_d(*D. melanogaster*) = 106 s^{-1}. We thus take the measured triplet decay constants for [ZnCcP, Fe^{2+}Cc] to be the intrinsic value, k_d, for ZnP incorporated into CcP.

For complexes of ZnCcP with Cc(WT) in 30% EG, k_d decreases smoothly from 126 (4) s^{-1} at 293 K to 66 (3) s^{-1} at 190 K. Following the protocol used with Zn-substituted Hb hybrids,[37a] the temperature dependence of k_d for each complex was fit to eq 1 in order to interpolate values for k_d to use in obtaining rate constants for the triplet quenching within the [ZnCcP, Fe^{3+}Cc] complexes:

$$k_d = k_1 \exp[-B/(RT)] + k_0 \quad (1)$$

The temperature dependence of the intrinsic decay constant for [ZnCcP, Fe^{2+}c(WT)] is well described by this equation with values of k_1 = 1.96 (0.72) × 10^5 s^{-1}, B/R = 2350 (110) K, and k_0 = 66.2 (1.7) s^{-1}. Among the various [ZnCcP, Fe^{2+}Cc] complexes, the fit parameters varied only slightly as follows: 5 × 10^5 s^{-1} ≥ k_1 ≥ 1 × 10^5 s^{-1}; 2750 K ≥ B/R ≥ 2200 K; 69 s^{-1} ≥ k_0 ≥ 62 s^{-1}. We conclude that, at all temperatures, k_d for [ZnCcP, Fe^{2+}Cc] is experimentally indistinguishable for the various Cc.[37b]

Equation 1 was used, in part because we anticipated that the intrinsic decay would involve contributions from repopulation of the singlet state, with an activation energy equal to the singlet–triplet gap of 8.40 kcal/mol. Although the intensity of the emission signal has an activated term, the activation energy (B) determined by fitting the temperature dependence of the decay rate, $k_d(T)$, to eq 1 (5.44 ≳ B ≳ 4.4 kcal/mol) is considerably less than the singlet–triplet energy gap. Rather, the magnitude of the activation energy is closer to the vibrational energy for porphyrin ring modes (1550 cm^{-1}),[38] suggesting that vibronic coupling in vibrationally excited molecules might be the source of the temperature-dependent term in eq 1.

Kinetics of Triplet Decay within Complexes of ZnCcP with Fe^{3+}Cc (Fungal). Quenching of the ^{3}ZnP in ZnCcP by Fe^{3+}P within Fe^{3+}Cc from fungi has been studied in 30% EG for the [ZnCcP, Fe^{3+}Cc] complexes prepared with Cc(WT) and Cc(*C. krusei*). At 293 K, the quenching rate constants are $k_q = k_p - k_d$ = 279 (16) − 126 (4) = 153 (16) s^{-1} for the former (Figure 6) and k_q = 130 (5) s^{-1} for the latter. In both cases, as the temperature is lowered to 250 K, k_q changes little, but upon further lowering the temperature the quenching vanishes in a transition that is centered at T_{mid} = 235 K with a width of only ~30 K (Figure 7). Outside of the transition range, the triplet decay traces for these [ZnCcP, Fe^{3+}Cc] complexes, like those for the [ZnCcP, Fe^{2+}Cc] complexes, are exponential for ≥5 half-lives (Figure 6). However, within the transition range (220 K ≤ T ≤ 250 K), heterogeneous kinetics are observed (Figure 6) and the decay traces are well described by a two-exponential kinetic equation:[39,40]

$$A = A_0[f \exp(-k_p t) + (1 - f) \exp(-k_s t)] \quad (2)$$

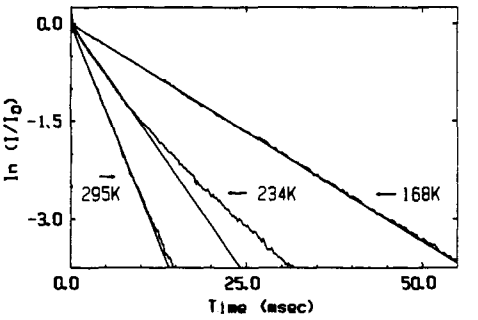

Figure 6. Time-resolved luminescence decays for the [ZnCcP, Fe^{3+}Cc(WT)] complex in 30% EG at 295, 234, and 168 K. Traces were fit with an exponential rate expression (k_{295} = 267 s^{-1}; k_{168} = 67 s^{-1}). For the trace at 234 K, only the first 10% of the data was fit to a single exponential rate equation (k = 165 s^{-1}). Conditions: 3.4 μM ZnCcP; 14.1 μM Cc; 30% EG/10 mM KPi, pH 6 cryobuffer.

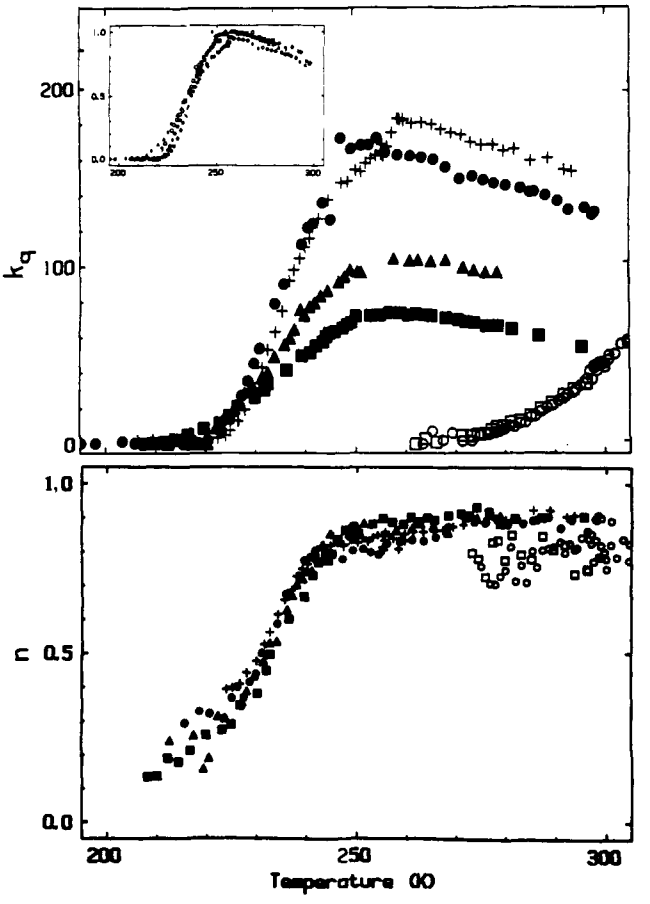

Figure 7. Temperature dependence of the triplet-state quenching parameters k_q (upper) and n (lower), from eq 3 for the [ZnCcP, Fe^{3+}Cc(WT)] complex in 15% (+), 30% (●), 45% (▲), and 60% (■) EG and for the [ZnCcP, Fe^{3+}Cc(horse)] complex in 30% (○) and 60% (□) EG. Inset: Rate constants are shown normalized to the maximum value for a given data set from the upper panel.

(35) Koloczek, H.; Horie, T.; Yonetani, T.; Anni, H.; Maniara, G.; Vanderkooi, J. M. *Biochemistry* **1987**, *26*, 3142–3148.

(36) In aqueous solvents, the triplet-state decay rate constant increases from 85 s^{-1} at −8 °C to 130 s^{-1} at −11 °C before decreasing to the same low-temperature plateau rate constant that is observed for the complexes with ferrous Cc. This sharp increase in k_d during freezing most likely results from intermolecular quenching.

(37) (a) Peterson-Kennedy, S. E.; McGourty, J. L.; Kalweit, J. A.; Hoffman, B. M. *J. Am. Chem. Soc.* **1986**, *108*, 1739–1746. (b) In general $k_d(T)$ was measured for each sample by reducing the Fe^{3+} Cc (see Materials and Methods). However, in some cases, k_d was calculated from a fit to eq 1 of the temperature dependence of k_d for a data set that combines decay rates for Cc(F82S), Cc(F82L), Cc(rat Y67F), and Cc(tuna), giving k_1 = 5.07 × 10^5 s^{-1}, B/R = 2750 K, and k_0 = 69.2 s^{-1}.

(38) Abe, M.; Kitagawa, T.; Kyogoku, Y. *J. Chem. Phys.* **1978**, *69*, 4526–4534.

When all four parameters (f, k_s, k_p, and A_0) are varied during the nonlinear least-squares fits with eq 2, the rate constant for the slow phase is nearly identical with the intrinsic decay rate constant, k_d. We thus fixed $k_s = k_d$ given by eq 1 to obtain values for f and k_p. This limit describes a partition between two forms of a complex: one, with fraction f, that exhibits quenching and one that does not.

As expected from the analysis of Marshall,[41] the nonexponential progress curves are equally well described with distributed kinetics. We have examined a model in which at any given temperature all complexes have the same intrinsic rate constant (k_d) and the quenching rate constant (k_q) is described by a stretched exponential:[42]

$$A = A_0 \exp[(-k_d t) - (k_q t)^n] \quad (3)$$

The distribution of rates implicit in this equation is described in detail by Lindsey and Patterson.[43] In the limit where $n = 1$, all complexes exhibit the same quenching rate constant, and eq 3 reduces to a single exponential. As n decreases, the breadth of the distribution in k_q increases and one may define an average rate constant ($k_{avg} = nk_q$). For $n \geq 0.2$, the most probable rate constant is within ~10% of k_q. The assignment of a unique k_d at any temperature incorporates the observation made with reduced complexes that the intrinsic decay rate (k_d) remains exponential down to 77 K and suggests that the nonexponential behavior for the [ZnCcP, Fe^{3+}Cc] complex is associated only with the quenching process.

Regardless of which fitting scheme (eq 2 or 3) was used,[44] the occurrence of a transition between 220 and 250 K in the triplet decay kinetics is clearly reflected in the parameters describing the decay traces. When using eq 2, k_p decreases smoothly while the fraction (f) decreases in a sigmoidal fashion from $f \approx 1$ to $f \approx 0$ through the transition range (see Figure 2A of ref 24). As seen in Figure 7, when the data are fit with the stretched-exponential equation, both the quenching rate (k_q) and the distribution parameter (n) decrease sharply during the transition. In any case, the nonexponential kinetics necessitate that, within the transition range, conformational interconversion is *slow* compared to the triplet decay rate. We now discuss some implications of the fits to eq 2; outside of this section, we discuss only the results obtained with eq 3.

The two-state model (eq 2) was used to test whether the slow phase with rate constant k_d corresponds to uncomplexed ZnCcP that appears because characteristics of the cryosolvent at low temperatures cause the equilibrium constant for complex formation [$K_a(T)$] to fall precipitously as the temperature is lowered through T_{mid}. This is shown to be unlikely by the instability of uncomplexed ZnCcP in cryosolvents and is ruled out[13] because within the transition range the fraction, $f(T)$, is unaffected by a 10-fold decrease in the ratio, $R = [Cc]/[CcP]$, whereas interpretation of this fraction in terms of an equilibrium between free and bound ZnCcP would predict a large shift in $f(T)$ for such a change in R.

Alternatively, the two-state model would apply if a low-temperature, inactive form of the complex were created by a change in ligation of either ZnP or FeP. However, the UV-vis and MCD data presented above (Figures 1-4) show the coordination spheres of the metal ions to be unchanged down to 4 K. Instead, we tentatively interpret the abrupt loss of quenching as signaling a transition in the interfacial docking geometry *within* the protein complex. This interpretation is congruent with data suggesting that the rate-limiting step for intracomplex ET near ambient temperatures may be a conformational conversion between inactive and active forms (conformational "gating").[45] The alternate possibility would be freezing of one or both proteins into a set of inactive conformational substates.[46]

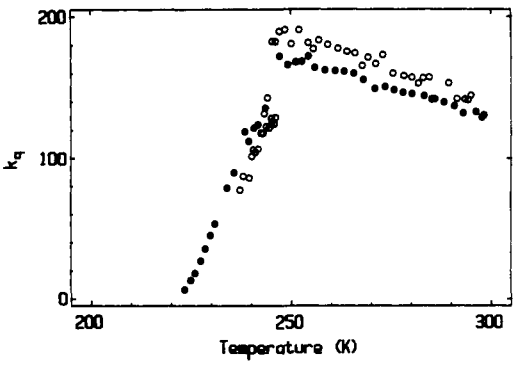

Figure 8. Temperature dependence of the triplet-state quenching rate constant (k_q) from eq 3 for the [ZnCcP, Fe^{3+}Cc(WT)] complex in 30% EG (●) and 30% GlOH (○). Conditions: 10 mM KPi, pH 6 buffer.

Solvent Effects. To determine whether the transition is "slaved" to the glassing transition of the solvent, we examined the temperature dependence of the quenching rate constant for [ZnCcP, Fe^{3+}Cc(WT)] in 15%, 30%, 45%, and 60% EG. Figure 7A shows the temperature response of k_q (from eq 3) in these solvents, the inset to Figure 7A shows k_q normalized to the maximum rate in each solvent (k_q/k_{max}), and Figure 7B shows the temperature dependence of the distribution parameter, n. The plots of k_q/k_{max} and of n as a function of temperature show that the midpoint and width of the transition are largely independent of the solvent composition and have about the same values for solutions that glass below T_{mid} (60% EG) as for those solutions that crystallize at a temperature comparable to (45% EG) or greater than (15% and 30% EG) T_{mid}.[24] This invariance with solvent composition indicates that the transition in k_q is an intrinsic phenomenon of the [ZnCcP, Fe^{3+}Cc] complex and is not slaved to the solvent, unlike CO rebinding to myoglobin.[46]

Further evidence that the transition is intrinsic to these complexes has been obtained by examining the temperature dependence of k_q by using different cryobuffers. Figure 8 shows the occurrence of a transition in the quenching rate for [ZnCcP, Fe^{3+}Cc(WT)] in 30% EG and 30% GlOH cryobuffers. Clearly, the transition in the triplet quenching rate is *not* unique to the EG solvent system, which corroborates the conclusion that it is not simply a solvent-driven phenomenon. However, the transition is not wholly insensitive to the environment of the complex; T_{mid} shifts slightly from 235 K for 30% EG to 240 K for 30% GlOH. Furthermore, one detects a small discontinuity in k_q at the freezing point ($T \approx 256$ K) for the 15% EG solvent (Figure 7A).

Although the transition range does not change with [EG], Figure 7A shows that, for $T > 250$ K, the quenching rate constant for the [ZnCcP, Fe^{3+}Cc(WT)] complex changes with [EG]. In particular, Figure 9 shows that, at ambient temperature, k_q for the [ZnCcP, Fe^{3+}Cc(*C. krusei*)] complex decreases smoothly as the percentage of EG increases: e.g., $k_q = 141$ (2) s^{-1} in aqueous buffer and $k_q = 19$ (2) s^{-1} in 70% EG. Below the transition range, quenching has been abolished and the triplet decay rate is independent of solvent, as observed with reduced complexes.

(39) Alcala, J. R.; Gratton, E.; Prendergast, F. G. *Biophys. J.* **1987**, *51*, 587-596.

(40) (a) Hoffman, B. M.; Ratner, M. A.; Wallin, S. A. In *Electron Transfer in Biology and the Solid State*; Johnson, M. K., et al., Eds.; American Chemical Society: Washington, DC, 1990; pp 125-146. (b) Hoffman, B. M.; Ratner, M. A. *J. Am. Chem. Soc.* **1987**, *109*, 6237-6243. Erratum: *J. Am. Chem. Soc.* **1988**, *110*, 8267.

(41) Marshall, D. B. *Anal. Chem.* **1989**, *61*, 660-665.

(42) Siebrand, W.; Wildman, T. A. *Acc. Chem. Res.* **1986**, *19*, 238-243.

(43) Lindsey, C. P.; Patterson, G. D. *J. Chem. Phys.* **1980**, *73*, 3348-3357.

(44) We also could reproduce the progress curves within the transition range using a Gaussian distribution of quenching rates, $G(k_{peak}, \sigma) = \exp[-(k - k_{peak})^2/\sigma^2]$. The fits yielded negative values for k_{peak} at $T \leq 230$ K. In this case, the physically relevant portion of $G(k_{peak}, \sigma)$ where $k \geq 0$ loses the features associated with a Gaussian distribution and becomes unsymmetrically skewed, rather like the distribution that gives rise to eq 3. Upon cooling, a sharp transition is apparent only in k_{peak}; the distribution parameter (σ) increases smoothly with cooling.

(45) (a) Wallin, S. A.; Stemp, E. D. A.; Everest, A. M.; Nocek, J. M.; Netzel, T.; Hoffman, B. M. *J. Am. Chem. Soc.* **1991**, *113*, 1842-1844. (b) Everest, A. M.; Wallin, S. A.; Stemp, E. D. A.; Nocek, J. M.; Mauk, A. G.; Hoffman, B. M. *J. Am. Chem. Soc.* **1991**, *113*, 4337-4338.

(46) Austin, R. H.; Beeson, K. W.; Eisenstein, L.; Frauenfelder, H.; Gunsalus, I. C. *Biochemistry* **1975**, *14*, 5355-5373.

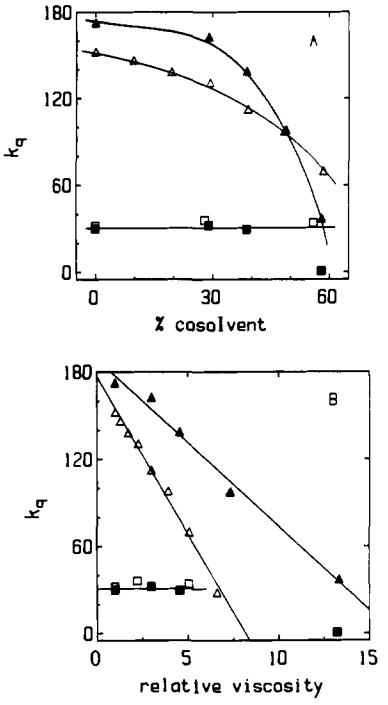

Figure 9. Effect of solvent composition on the quenching rate constant (k_q) for the [ZnCcP, Cc(*C. krusei*)] and [ZnCcP, Cc(horse)] complexes. (A) Plot of k_q vs solvent composition; lines are only to guide the eye. Conditions: [2 μM ZnCcP, 7 μM Cc(*C. krusei*)] in EG (△) and GlOH (▲); [1–2 μM ZnCcP, 4–7 μM Cc(horse)] in EG (□) and GlOH (■). Except for the measurements with the [ZnCcP, Cc(*C. krusei*)] complex in GlOH, all cryosolutions were buffered at pH 6; for the latter, the solutions were buffered at pH 7. (B) Replot of the data in the upper panel as a function of the relative viscosity of the solvent. Viscosity values were interpolated from tables in *CRC Handbook of Chemistry and Physics*, 60th ed.; Weast, R. C., Ed.; CRC Press, Inc.: Boca Raton, FL, 1980; D237–D240. The viscosity of the buffer is taken to be equivalent to the absolute viscosity of water at 20 °C (1.002 cP). The solid line is an empirical fit of the relative viscosity dependence of k_q to $k_q = A\eta^\circ + B$. For EG, $A = -21.7\ s^{-1}$ and $B = 177\ s^{-1}$; for GlOH, $A = -11.5\ s^{-1}$ and $B = 188\ s^{-1}$.

The most obvious sources of this inverse variation of k_q with cryosolvent concentration at temperatures greater than ~250 K would be a response of the quenching rate constant either to the increase in the solvent viscosity or the decrease in the dielectric constant of the solvent. The quenching rate constant for [ZnCcP, Fe^{3+}Cc(*C. krusei*)] is found empirically to decrease linearly with viscosity (Figure 9, right). To further explore this, we measured the decay rate constant as a function of [GlOH], which has a larger range in viscosity. As with the measurements in EG, we find that the quenching rate constant decreases linearly with viscosity. Such a strong correlation clearly suggests that the rate constant is indeed responding to viscosity, and a full investigation is in progress.

Kinetics of Triplet Decay in Complexes with Nonfungal and Mutant Cc. To explore the structural basis for the transition in k_q, we have studied triplet quenching in complexes with Cc from nonfungal sources as well as complexes with Cc(yeast iso-1) in which the phenylalanine of position 82 is modified by site-directed mutagenesis, Cc(F82X). Both the solvent dependence of k_q at ambient (Table I) and the temperature dependence of the quenching rates (Figure 10) show that the complexes investigated fall into two classes.

Class I includes the complexes with the Fe^{3+}Cc from *C. krusei* and *D. melanogaster*, as well as those with a suite of position 82 mutants of Cc(yeast iso-1) [Phe(WT), Ser, Leu, Ile, and Met]. For each of these Cc, the quenching rate constant within the [ZnCcP, Fe^{3+}Cc] complex shows the transition near 250 K (Figure 10), and in each case the quenching rate constant at ambient temperature decreases sharply with increasing viscosity (Table I). For a given solvent, the quenching rate constant (k_q from eq 3) varies substantially among these Cc. For temperatures above and through the transition, k_q decreases in the order Cc(*C. krusei*), Cc(WT) ≥ Cc(F82M) ≥ Cc(F82S) ≥ Cc(F82L), Cc(F82I) ≥ Cc(*D. melanogaster*) (Table I, Figure 10). However, the shape of the decay curve at each temperature as measured by the distribution parameter n (eq 3) is essentially the same for all the complexes within this class (data not shown). Furthermore, the temperature response of k_q/k_{max} is remarkably similar for all these Cc (Figure 10, lower), and the midpoint of the transition varies only slightly ($235\ K \le T_{mid} \le 244\ K$; Table I). These results indicate that, at any temperature within the transition range, the average rate constant varies among the different complexes, but the shape of the distribution of rate constants is the same. This further confirms that the transition is dependent upon the protein structure rather than the solvent.

Table I. Solvent Dependence of the Triplet-State Quenching Rate Constant (k_q)[a]

C_c	k_q(293 ± 2 K) 0% EG	30% EG	60% EG	T_{mid} (K)
yeast iso-1[b]				
WT (F82)	150[c,d]	157	72	235
F82M	141	116		243
F82S	172	95	32	244
F82L	89	86	26	244
F82I	30[c]	43		243
D. melanogaster		48		239
C. krusei	152[d,e]	131[d,e]	70[d,e]	241
horse	25	30	31	na
tuna	30	7		na
rat		27		na
rat (Y67F)		19		na

[a] 10 mM KPi, pH 6; k_q obtained from fits to an exponential decay function by using $k_d = 115\ s^{-1}$ (see text). T_{mid} is the midpoint of the transition in cryobuffer. Errors: k_q, ±10%; T_{mid}, ±3 K. [b] Each protein carries a background (C102T) mutation. [c] 1 mM KPi, pH 7. [d] k_q obtained from transient absorption experiments at 475 nm. [e] 10 mM KPi, pH 7.

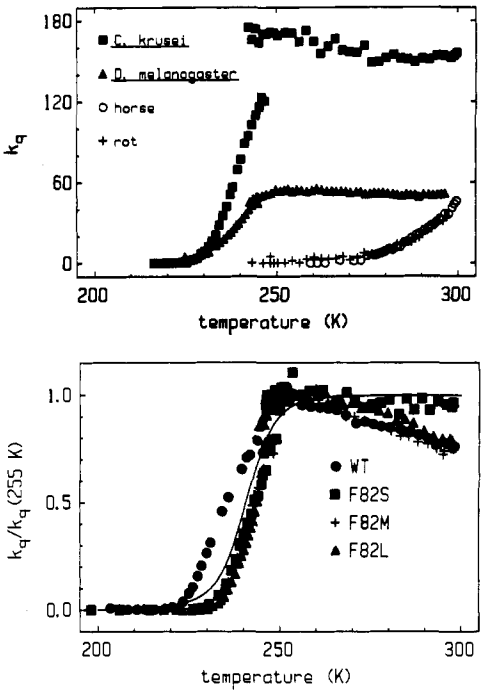

Figure 10. Temperature dependence of k_q from eq 3 for complexes of ZnCcP with Cc from several species (upper) and a suite of Cc(F82X mutants) (lower) in 30% EG/10 mM KPi, pH 6 cryobuffer. Lower: The quenching rate constants have been normalized as in the inset to Figure 7 relative to the rate constants at 255 K, Cc(F82S), 121 s^{-1}; Cc(F82M), 155 s^{-1}; Cc(WT), 172 s^{-1}; and Cc(F82L), 100 s^{-1}. The solid line is a fraction of broken bonds obtained as described in ref 58; the parameters employed are given in the text.

The Cc from horse, rate, and tuna form a second class of complexes with quite different properties. At every temperature, the triplet state decay curves for this second group of complexes show essentially exponential kinetics and k_q is virtually the same for each of the three Cc (Table I). The quenching rate constant is low at room temperature [$k_q \approx 25\ s^{-1}$] (Figures 7 and 10; Table I) and decreases smoothly to $k_q \approx 0$ by 270 K (Figures 7 and 10). The temperature dependence of k_q fits well to an Arrhenius function with an activation energy, $E_a = 3.75$ kcal/mol. The two classes of complexes differ dramatically in the response of the triplet quenching rates to addition of EG to the solvent. Whereas k_q for the class I complexes decreases strongly as [EG] increases, Figures 7 (upper), 9, and 10 and Table I show that k_q for the [ZnCcP, Fe^{3+}Cc(horse)] complex is independent of [EG] at all temperatures.

Inspection of Figures 7 and 10 suggests that the transition seen with the class I complexes has been shifted for the [ZnCcP, Fe^{3+}Cc(horse)] complex and that the quenching at $T \geq 270$ K might be the low-temperature portion of a broad transition with $T_{mid} \geq 300$ K. The invariance of k_q with solvent composition might then correspond to the solvent independence of k_q for class I complexes when $T \ll T_{mid}$. In opposition to this idea, the kinetic traces for the [ZnCcP, Fe^{3+}Cc(horse)] complex are effectively single-exponential at all temperatures. This is consistent with the occurrence of a transition only if the interconversion rates at these higher temperatures are *fast* compared to the triplet decay rates.

To test whether T_{mid} is indeed shifted for the complex with Cc(horse), we extended our kinetic measurements for this complex above ambient. The quenching rate remains exponential and continues to climb, reaching a value of 109 s^{-1} at 323 K; above this temperature, the protein complex is unstable.[47] Because no inflection point is seen by 323 K, the correspondence between the transition for class I complexes and that in the [ZnCcP, Fe^{3+}-Cc(horse)] complex cannot be confirmed. More likely, different phenomena are being observed with the two classes. What is definitive is that the two types of complexes behave quite differently.

Discussion

We have shown that a set of [ZnCcP, Fe^{3+}Cc] complexes undergo a sharp transition in the range 220 K < T < 250 K between a low-temperature state that does not exhibit triplet quenching and a high-temperature state that does. Within this narrow transition range, the triplet-state decay traces for the [^{3}ZnCcP, Fe^{3+}Cc] complexes are nonexponential, and outside of this range they are exponential. The quenching rate constants vary strongly among complexes with different Cc, and above 250 K they decrease sharply with [EG]. However, both the midpoint and the breadth of the transition remain constant within this class. Elsewhere[48] we show that, for $T \geq 260$–270 K, the triplet-state quenching within these complexes exhibits both electron and energy transfer components, with the partitioning between these depending on the Cc. However, below this temperature, energy transfer dominates, and the quenching rate constant can be discussed in terms of the structural and spectral factors that determine the rate constant for Förster energy transfer.[49] We have ruled out trivial explanations for the abrupt change in kinetics, such as the following: changes in metal coordination state that would lead to changes in the ZnCcP emission spectrum and/or loss of the 695-nm band of Cc, thereby producing changes in the spectral overlap required for Förster energy transfer; dissociation of the complex. Further, we have presented evidence that this process is not solvent-driven. Thus, we tentatively interpret these observations as signaling a transition in the interfacial docking geometry *within* the protein complex.

Several reports of conformationally gated ET provide precedence for the inference that quenching within [ZnCcP, Fe^{3+}Cc-(class I)] complexes involves physical reorientation of the redox partners. The reaction of Cc(horse) with photosynthetic reaction center proteins was interpreted with a model invoking conformational gating;[50] Moser and Dutton found that, in low ionic strength media, the rate of the conformational transition of Cc from the "distal" binding site to the "proximal" site shows an *inverse* dependence on viscosity, while the reverse reaction was found to be independent of viscosity, and it was inferred from this behavior that translational and/or rotational diffusion are involved in the stabilization of the redox-active proximal state. The inverse dependence of k_q on viscosity for the complex between ZnCcP and the Cc from *C. Krusei* (Figure 9) or yeast (see Figure 7) similarly indicates that solvent "friction" on intracomplex motions influences the quenching reaction. Note, however, such effects of friction are known to manifest themselves in activated processes as well as in diffusional ones.[50b] Conformational gating has also been invoked to explain the kinetic observations for the reduction of CcP compound ES within its complex with Fe^{2+}Cc[3a] and for the ET from Fe^{2+}CcP to Fe^{3+}Cc.[3b]

Some of the complexes studied here (class I) show the low-temperature transition, and others do not (class II). The computer modeling results with the [Fe^{3+}CcP(yeast), Fe^{3+}Cc(yeast iso-1)][51] and [Fe^{3+}CcP(yeast), Fe^{3+}Cc(tuna)] complexes[5] provide a global comparison of the structures of the two classes of complexes. We see that the metal–metal distance has increased from 23 Å in the complex with Cc(yeast iso-1) to 23.8 Å in the complex with Cc(tuna), and the interfacial contact distance between two of the residues thought to provide a hydrophobic binding interaction, Phe 82 (Cc) and His 181 (CcP), is 3.3 Å shorter while the heme groups are more nearly parallel for the [CcP, Cc(yeast)] complex than for the [CcP, Cc(tuna)] complex. The [CcP, Cc] protein interface, unlike that in mixed-metal hemoglobin hybrids,[37] is accessible to the solvent, and the strong dependence of the quenching rate constant on solvent likely reflects this fact. Differing extents of solvent accessibility may also help to regulate the docking geometry by shielding surface charges that are involved in the formation of salt bridges between the two proteins. It is conceivable that subtle changes such as these "customize" the geometry of the complex.

To help understand the structural basis for the division of the Cc into two classes and thus the structural basis for the transition, we have compared the primary sequences of the species of Cc that have been studied (Table II). All of the Lys residues of Cc thought to be involved in docking (Lys 13, 27, 72, 86, and 87) are conserved, with the exception of Lys 13, which is replaced by an Arg residue in both Cc(*D. melanogaster*) and the proteins from yeasts. Phe 82, likewise, is conserved among all the species we studied. Despite the fact that Cc(*D. melanogaster*), like Cc(rat) and Cc(horse), is only ~60% homologous with Cc(yeast iso-1) and its quenching rate constant at ambient within the [ZnCcP, Fe^{3+}Cc] complex is low, like that for [ZnCcP, Fe^{3+}Cc(class II)] complexes, the quenching rate for the [ZnCcP, Fe^{3+}Cc(*D. melanogaster*)] complex undergoes the same conformational tran-

Table II. Amino Acid Residues of Cc(*D. melanogaster*) That Are Unique or Common with Cc(Yeast iso-1) but *not* Cc(Horse)

residue number[a]	Cc(yeast iso-1)	Cc(*D. melanogaster*)	Cc(horse)
9	Leu	Leu	Ile
13	Arg	Arg	Lys
28	Val	Val	Thr
36	Phe	Ile	Phe
85	Leu	Leu	Ile

[a] Residues are numbered relative to the sequence of Cc(tuna); amino acid sequences are from *The Protein Identification Resource* (June 30, 1990, Release No. 25.0). Protein Sequence Data Base (Natl. Biomed. Res. Found., Washington, DC).

(47) Kresheck, G. C.; Erman, J. E. *Biochemistry* **1988**, *27*, 2490–2496.
(48) Nocek, J. M.; Hoffman, B. M. Manuscript in preparation.
(49) Förster, T. *Discuss. Faraday Soc.* **1959**, *27*, 7–17.
(50) (a) Moser, C. C.; Dutton, P. L. *Biochemistry* **1988**, *27*, 2450–2461. (b) Fleming, G. R.; Wolynes, P. G. *Phys. Today* **1990**, 36–43.
(51) Lum, V. R.; Brayer, G. D.; Louie, G. V.; Smith, M.; Mauk, A. G. *Protein Structure, Folding, & Design 2*, UCLA Symp. on Molecular & Cellular Biology, New Series, 69; Oxender, D. L., Ed.; Alan R. Liss: New York, 1987; pp 143–150.

sition that is observed with the [ZnCcP, Fe^{3+}Cc(class I)] complexes. Surprisingly, there are only four amino acid residues (Leu 9, Arg 13, Val 28, and Leu 85) that the Cc(*D. melanogaster*) protein shares with Cc(yeast iso-1) *but* not with either Cc(rat) or Cc(horse), and one residue (Ile 36) that is unique to Cc(*D. melanogaster*) (Table II). Except for position 36, all of these positions are in close proximity to the interface, and only position 28 is a nonconservative change. Indeed, position 13 has been suggested as one of the residues involved in the docking of Cc to its redox partners, and Hazzard et al.[52] found that mutation of Arg 13 to Ile increased the rate for intramolecular ET from Fe^{2+}Cc to compound ES at low ionic strength. This suggests that interaction of Lys 13 with CcP might actually favor the docking of the proteins in an inactive geometry. Replacement of the polar residue at position 28 [Val 28 in Cc(yeast iso-1)] with a nonpolar residue [Thr 28 in Cc(*D. melanogaster*)] could influence the electrostatic interactions in the complex, as its neighbor is Lys 27, which is involved with complexation. Even the changes in the primary structure at positions 9 and 85, which involve a conservative replacement (Leu with Ile), may influence the kinetics for the quenching process as they require different "packing restraints" with CcP. At any rate, these observations suggest specific residues for further mutagenesis studies that might be useful for testing the functional role of interfacial contacts.

Phe 82 is an evolutionarily conserved residue within the interfacial region that has long been believed to be important for anchoring Cc to its redox partners.[53] Changing only this one amino acid residue in Cc(yeast iso-1) produces nearly as large of an effect on the triplet decay rate as does the use of Cc(*D. melanogaster*), which differs from Cc(yeast iso-1) at ~40% of its amino acid residues. The Cc(F82I) and Cc(F82L) mutants have been shown to bind more tightly to cytochrome *c* oxidase than does the wild type protein.[54] As it is known that Cc uses the same surface domain for interactions with both cytochrome *c* oxidase and CcP,[55] it might be expected that a tighter complex should impede the reorientation process thought to be involved in the transition. The variation in the quenching rate constants may reflect these differences in binding.

Cooperative Binding Model. The observation of nonexponential kinetics within the transition range is consistent with the presence of two or more states that interconvert at a rate that is less than, or competitive with, the quenching process. The decay traces are equally well described with either a discrete two-state distribution of states or with the continuous distribution implied by the stretched exponential kinetic expression. In either case, there are two physical interpretations for these kinetic observations. The first is that the transition reflects a change in the equilibrium distribution of slowly interconverting forms of the complex, "complexomers". The second is that there is a progressive change in the interconversion rates within the transition range. Both raise the question: How can a system of two interacting proteins exhibit such a sharp "phase transition"?

We begin with the idea that, at ambient temperatures, the [CcP, Cc] complex undergoes rapid rearrangements. Further, one (or more) subset(s) of the accessible complexomers exhibits triplet quenching, but the most thermodynamically stable set of complexomers does not. Below the transition range, the complex exists in the latter forms; as the temperature is raised, a transition to the quenching forms results from loosening of the interface.

Simple Arrhenius treatment of the temperature dependence of the quenching rate constant, k_q (eq 3), for [ZnCcP, Fe^{3+}Cc] within the transition region leads to a surprisingly large activation energy (E_a = 38.0 kcal/mol). Alternatively, the fraction of conformers exhibiting quenching assuming a two-state distribution is $f(T) = K(T)/[1 + K(T)]$ where $K(T)$ is the equilibrium ratio

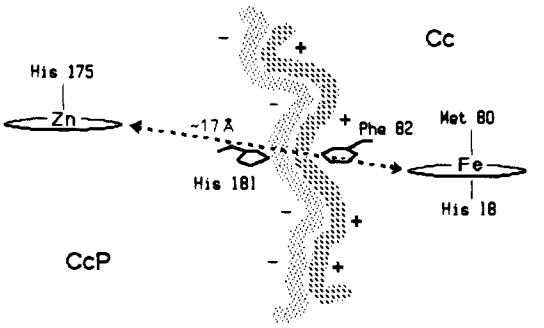

Figure 11. Schematic representation of the interface of the [ZnCcP, Cc] complex.

of active to inactive complexomers. A fit to these data does not give so large an enthalpy change (ΔH = 15.5 kcal/mol) but instead gives a very large entropy change (ΔS = 68.8 eu; this large positive value is the motivation for the idea that the majority of the complexomers exhibit quenching). The large apparent values for E_a and/or ΔS, along with the sigmoidal shape of the temperature dependence of the fraction (eq 2), visually suggest that the transition between the active and inactive states is a cooperative process. The intraprotein transitions among substates seen in studies of CO recombination to hemoproteins at low temperatures[46] is perhaps analogous, although in this case the transition is thought to be solvent-driven. We present the following heuristic description of the transition as a basis for thought and future experiment.

Consider the representation of the [CcP, Cc] interface shown in Figure 11. It contains salt bridges and a hydrophobic interaction such as those postulated by Poulos and Kraut in their docking model.[5] This picture immediately suggests that the formation of such an array of bonds would be a cooperative process, in analogy to the cooperative formation of the linear array of hydrogen bonds that underlies the helix–coil transition in polyamino acids. At low temperatures, the energetics favor formation of all the bonds as shown in Figure 11. At high temperatures, the entropic price of bond nucleation leads to a disorganization of the interface. The organized (low-temperature) complex corresponds formally to the helix form of a polyamino acid; the disorganized (high-temperature) complex corresponds to the coil. A detailed model for the transition of course should consider that the high-temperature ("coil") state also must have some bonding of its own, or else there would be no complex. We do not try to model the high-temperature form of the complex, nor do we refine the picture by addressing the differences between hydrophobic and hydrophilic interactions[56] or by closing the bonds into a ring to better model the interface. We simply use this picture to ask whether a protein–protein complex that is bound by a relatively *small* number of interactions might exhibit a thermal transition as sharp as that of Figures 7, 8, and 10.

In discussing the helix–coil transition, Davidson[57] presents a statistical mechanical treatment of a unidimensional array of N bonds that is formally equivalent to the representation in Figure 11, which has N = 5. This treatment is characterized by (1) the thermodynamic parameters of bond formation written as $S = S_0 \exp(-\epsilon/RT)$ where $S_0 < 1$ is related to the entropy loss per bond formed and $\epsilon < 0$ is the energy gained upon bonding and (2) a nucleation parameter, $\sigma \ll 1$, for the formation of a bond whose neighboring bond is broken. Davidson shows that this model can provide cooperative helix–coil transitions for $N \approx 10^3$; can it do so for, say N = 5 with reasonable thermodynamic values? The answer is that almost *any* reasonable guess for the parameters produces a transition that is qualitatively similar to that observed with the [ZnCcP, Cc] complexes. For example, in Figure 10, we compare the temperature dependence of k_q/k_{max} (eq 3) for the complexes of ZnCcP with Cc(F82X) with the temperature dependence of the average fraction of broken bonds[58] for our linear,

(52) Hazzard, J. T.; McLendon, G.; Cusanovich, M. A.; Das, G.; Sherman, F.; Tollin, G. *Biochemistry* **1988**, *27*, 4445–4451.
(53) Louie, G. V.; Pielak, G. J.; Smith, M.; Brayer, G. D. *Biochemistry* **1988**, *27*, 7870–7876.
(54) Michel, B.; Mauk, A. G.; Bosshard, H. R. *FEBS Lett.* **1989**, *243*, 149–152.
(55) Bechtold, R.; Bosshard, H. R. *J. Biol. Chem.* **1985**, *260*, 5191–5200.
(56) Murphy, K. P.; Privalov, P. L.; Gill, S. J. *Science* **1990**, *247*, 559–561.
(57) Davidson, N. *Statistical Mechanics*; McGraw-Hill Book Co., Inc.: New York, 1962; pp 385–393.

cooperative complex calculated with the parameters $\epsilon_b = -4500$ cal/mol, $S_0 = 1.6 \times 10^{-4}$, and $\sigma = 3.2 \times 10^{-3}$. For illustrative purposes, we may define an entropy of nucleation, $\Delta S_n = R \ln \sigma = -11.4$ eV and an entropy of bond formation, $\Delta S_b \equiv R \ln S_0 = -17.3$ eu. The model with $N = 5$ and these parameters obviously generates a cooperative melting curve that closely mimics the transition reported here (Figures 7, 8, and 10). Within the spirit of this model, the parameters do not violate reasonable ideas of the strength of the entropy change for localizing opposing segments of the interface.

(58) The fraction of broken bonds is defined as $(\langle N(0)\rangle - \langle N(T)\rangle)/\langle N(0)\rangle$, where $\langle N(T)\rangle$ is the average number of bonds and is given by eqs 16-93 of ref 57 and $N(0) = N - 1$ in the model as formulated (ref 57). We have explored a range of N and find this makes no difference to the qualitative features of this approach. However, the magnitudes of ϵ_b, ΔS_b, and ΔS_n decrease with increasing N.

Future work will address such features as the structural differences that cause the high-temperature forms of the complex to exhibit quenching whereas the low-temperature form(s) do not. It will further seek a realistic picture of the interfacial interactions in both types of forms, as well as a kinetic mechanism that embodies the ideas proposed here.

Acknowledgment. We acknowledge research support from the NSF (Grant DMB 8907559 to B.M.H.), the NIH (Grants HL13531 to B.M.H.; GM 33806 to M.K.J.; GM 29001 and GM 19121 to E.M.), and the MRC of Canada (Grant MT-1706 to M.S.). We are indebted to Profs. John Torkelson and Laszlo Lorand for the gracious use of their spectrofluorimeters and to Drs. Sten Wallin, Eric Garber, and Thomas Luntz for helpful discussions.

Registry No. Cc, 9007-43-6.

Direct Evidence of a Bipolaron Charge Carrier in Conducting Polyazines from ^{13}C and ^{15}N Solid-State NMR Spectroscopy: Detection of a Nitrenium Cation by Natural Abundance ^{15}N Solid-State NMR Spectroscopy

Benjamin Chaloner-Gill,[†] William B. Euler,*[,†] Paul D. Mumbauer,[‡] and James E. Roberts*[,‡]

Contribution from the Departments of Chemistry, University of Rhode Island, Kingston, Rhode Island 02881, and Lehigh University, Seeley G. Mudd Building 6, Bethelehem, Pennsylvania 18015. *Received January 25, 1991*

Abstract: Natural abundance ^{13}C and ^{15}N solid-state NMR experiments were performed on undoped and doped samples of polyazine, $(-N{=}C(R){-}C(R){=}N-)_x$. The topology of the polymer requires that doping-induced charge carriers must be either polarons (radical cations) or bipolarons (dications). Magnetic susceptibility measurements shows that the iodine-doped polymers are diamagnetic, so the charge carriers must be bipolarons. The specific bipolaron charge carrier in polyazines has been identified; the nitrogens bear the charge primarily in the form of a nitrenium cation. This is the first report of a nitrenium cation detected by ^{15}N solid-state NMR spectroscopy. Independent of the substitution of the polyazine, R = H or CH_3, the same charge carrier is present.

Introduction

The field of conducting polymers has generated tremendous interest in the past decade.[1] The prototype conducting polymer is polyacetylene,[2-13] which has alternating double and single bonds along the all-carbon backbone. Analogous to polyacetylene is polyazine, $(-N{=}C(R_1){-}C(R_2){=}N-)_x$, which emulates polyacetylene but inserts an azine bond, $=N{-}N=$, at every other diene site. Unlike polyacetylene, polyazines are not oxidized in air. The presence of the heteroatom also likens polyazine to other heteroatom-containing conducting polymers: polypyrrole,[14-18] polythiophene,[19-26] and polyaniline.[27-36]

The oxidation (doping) of polymers with halogens has been widely used since polyacetylene was doped with iodine to give high levels of conductance.[37] The same behavior is seen in polypyrrole.[18] Permethylpolyazine doped with iodine only shows conductance levels similar to those of a semiconductor, with its highest level of conductance being 10^{-1} S cm^{-1}.[37] Examination of the spectroscopy should indicate what type of charge carrier is present within each polymer system. In this work, we present details of the NMR spectra of iodine-doped polyazines.

If the ^{13}C NMR spectra of an undoped and a doped polymer (or a nonconductive and a conductive form) are compared, no-

* Authors to whom correspondence may be sent.
† University of Rhode Island.
‡ Lehigh University.

(1) Skotheim, T. J. *Handbook of Conducting Polymers*; Marcel Dekker: New York, 1986.
(2) Fincher, C. R., Jr.; Ozaki, M.; Heeger, A. J.; MacDiarmid, A. G. *Phys. Rev. B* **1979**, *19*, 4140.
(3) Su, W. P.; Schrieffer, J. R.; Heeger, A. J. *Phys. Rev. Lett.* **1979**, *42*, 1698.
(4) Chien, J. C. W.; Wnek, G. E.; Karasz, F. E.; Hirsch, J. A. *Macromolecules* **1981**, *14*, 479.
(5) Baughman, R. H.; Moss, G. *J. Chem. Phys.* **1982**, *77*, 6321.
(6) Baughman, R. H.; Murthy, N. S.; Miller, G. G.; Shacklette, L. W. *J. Chem. Phys.* **1983**, *79*, 1065.
(7) Manenschijn, A.; Duijvestijn, M. J.; Smidt, J.; Wind, R. A.; Yannoni, C. S.; Clarke, T. C. *Chem. Phys. Lett.* **1984**, *112*, 99.
(8) Jeyadev, S.; Conwell, E. M. *Phys. Rev. B* **1986**, *33*, 2530.
(9) Chien, J. C. W.; Schen, M. A. *Macromolecules* **1986**, *19*, 1042.
(10) Basescu, N.; Liu, Z. X.; Moses, D.; Heeger, A. J.; Naarmann, H.; Theophilou, N. *Nature* **1987**, *327*, 403.
(11) Roth, S.; Bleier, H. *Adv. Phys.* **1987**, *36*, 385.
(12) Naarmann, H.; Theophilou, N. *Synth. Met.* **1987**, *22*, 1.
(13) Swager, T. M.; Dougherty, D. A.; Grubbs, R. H. *J. Am. Chem. Soc.* **1988**, *110*, 2973.
(14) Brēdas, J. L.; Scott, J. C.; Yakushi, K.; Street, G. B. *Phys. Rev. B* **1984**, *30*, 1023.
(15) Devreux, F.; Bidan, G.; Syed, A. A.; Isintavis, C. *J. Phys. (Paris)* **1985**, *46*, 1595.

0002-7863/91/1513-6831$02.50/0